Int. J. Solids Structures Vol. 29, No. 24, pp. 3113-3123, 1992
Printed in Great Britain.

0020-7683/92 $5.00 + .00

CRACK GROWTH AT INTERFACES IN BIMATERIAL SYSTEMS AND COMPOSITES

D. B. POPEJOY, L. R. DHARANI and H. TANG†
Department of Mechanical and Aerospace Engineering and Engineering Mechanics, University of Missouri-Rolla, Rolla, MO 65401, U.S.A.

(*Received* 18 *January* 1992; *in revised form* 3 *June* 1992)

Abstract—The problem of a crack impinging upon an interface between dissimilar materials is investigated using a Consistent Shear-Lag (COSL) model. The primary question to be answered is whether the crack will cross (penetrate) the interface or be deflected along it. Typically the stress and displacement fields in the vicinity of an interface create computational difficulties, especially when the elastic moduli of the adjacent regions vary greatly. The COSL model is modified to include a finite thickness interlayer region representing the interface to act as a buffer. The energy release rates for both deflected and penetrating cracks are determined. The ratio of these two quantities is then compared to that of debond and Mode I toughnesses to investigate the two scenarios for crack extension. The effect that elastic mismatch has on the energy release rates, and hence the mode of crack extension, is investigated. These results compare favorably with analytical solutions for semi-infinite domain bimaterial problems. The effect of anisotropy is investigated to determine the relative importance of the effect of elastic constants on the energy release rate ratio. It is shown that of these, the longitudinal and transverse elastic moduli are of greatest significance. This model is applied to cracks impinging on fiber–matrix interfaces in composite materials, and it is shown that the fiber volume fraction actually has little effect on the ratio of energy release rates.

1. INTRODUCTION

The primary purpose of this paper is to investigate the growth of cracks impinging upon material interfaces. More specifically, for a crack growing perpendicular to such an interface, it is of great importance to predict whether the crack will penetrate the interface or deflect into the interface. This problem has many practical applications, ranging from very small scale such as the fiber–matrix interface in a fiber-reinforced composite, to relatively large scale as in the cladding-fuel rod interface in a nuclear reactor. In the former application, it is often useful to consider a crack within the matrix material impinging upon a fiber. For the crack to continue to propagate, it can either penetrate the interface and break the fiber, or deflect into the interface and cause debonding. In the case of the cladding-fuel rod interface of a nuclear reactor, the determination of crack penetration/deflection is of practical concern. Crack deflection at the interface can lead to a separation of the cladding from the fuel rod, which can create a localized degradation of heat transfer characteristics. On the other hand, crack penetration of the interface can eventually lead to crack extension through the cladding to the primary coolant.

Several investigators have treated the crack penetration/deflection problem specifically for the case of bimaterials. By restricting the problem to bimaterials, He and Hutchinson (1989a) presented analytical solutions for cracks impinging perpendicularly on the interface between two semi-infinite regions. Goree and Venezia (1977a, b) also studied the bimaterial problem by considering both interfacial debonding and penetration. In addition, others have given analytical results for bimaterial systems in which cracks are present within the interface, including He and Hutchinson (1989b), Raju *et al.* (1987), Rice (1988), Sun and Manoharan (1989) and Yang (1991). In order to study more complex material systems, such as fiber-reinforced composites, the Classical Shear-Lag (CLSL) model has been used by Hedgepeth (1961), Goree and Gross (1979), Dharani *et al.* (1983), Nairn (1988) and Nairn *et al.* (1991). It should be noted, however, that the CLSL model makes the simplifying assumptions that the fibers only support normal stresses and the matrix only supports shear stresses. These assumptions are reasonable when the CLSL model is applied to composites in which the fibers are much stiffer than the matrix, such as in graphite–epoxy composites.

† Present address: Modern Engineering, Warren, MI 48092, U.S.A.

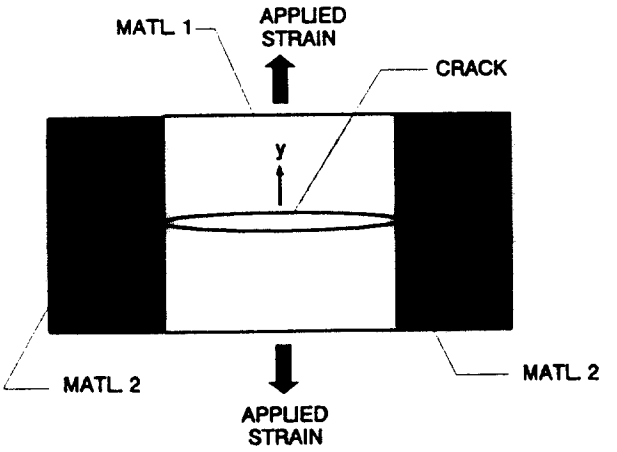

Fig. 1. Geometry of center-cracked symmetric bimaterial system.

On the other hand, such assumptions cannot be justified for metal–matrix composites (MMCs) as well as ceramic–matrix composites (CMCs) because the fibers and matrix possess comparable stiffnesses. Because of this, normal stresses must be included within the matrix material as well as shear stresses within the fibers. Thus, to accurately model the behavior of stiff matrix composites such as MMCs and CMCs, it is necessary to resort to a more broadly based model such as the Consistent Shear-Lag (COSL) model used by Dharani and Tang (1990), Dharani and Recker (1991) and Chai and Dharani (1991). It is important to note that the CLSL model as used by Nairn (1988) is highly specialized since it requires the fibers to be of uniform size and spacing. In this respect, the COSL model offers a distinct advantage since it allows for fibers which are non-uniformly spaced. In addition, the COSL model allows for anisotropic properties in each constituent, thus making it possible to more accurately model the behavior of certain materials.

2. FORMULATION

The geometry of the region containing the crack and subjected to a uniform strain ε_0 in the y direction is shown in Fig. 1. One advantage of the COSL model (Dharani and Tang, 1990; Chai and Dharani, 1991) is that it allows for heterogeneity on both sides of the interface so that materials 1 and 2 may each consist of several layers of different orthotropic materials. Owing to symmetry of the plate about both the x and y axes, the problem can be simplified somewhat by considering only one quarter of the region. When the crack tip reaches the material interface, it can either penetrate or deflect into the interface as shown in Fig. 2.

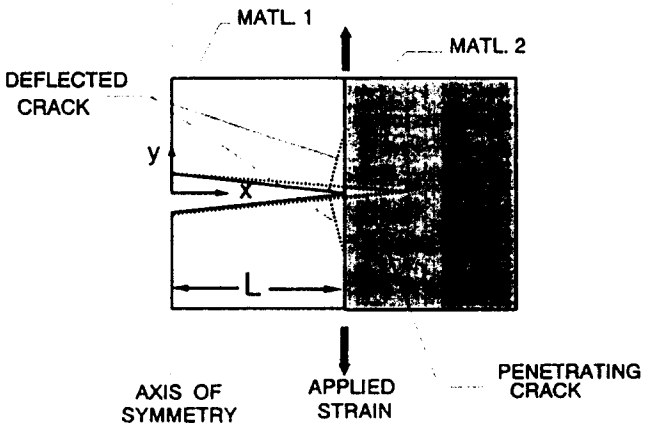

Fig. 2. Geometries of penetrating and doubly-deflected cracks.

To predict whether the crack will penetrate the interface or deflect into it, an energy release rate approach will be used. He and Hutchinson (1989a) postulate that the crack will deflect if

$$\frac{G_{ic}}{G_c} < \frac{G_d}{G_p}, \tag{1}$$

where G_d denotes the energy release rate of the deflected crack, G_p denotes the energy release rate of the penetrating crack, G_{ic} is the interfacial toughness, and G_c is the Mode I toughness of the material ahead of the crack tip. Otherwise, the crack will penetrate the interface and may continue to grow self-similarly.

2.1. *Consistent shear lag*

To implement the COSL model (Dharani and Tang, 1990; Chai and Dharani, 1991), the region shown in Fig. 1 must first by divided into N nodal elements. Figure 3 shows a typical element of finite width h and infinitesimal height dy. From equilibrium, the following equations can be derived:

$$\sigma_x^{(n+1/2)} - \sigma_x^{(n-1/2)} + \frac{h}{2}\left[\tau_{yx,y}^{(n+1/2)} + \tau_{yx,y}^{(n-1/2)}\right] + \delta_{n1}\left[\sigma_x^{(n-1/2)} - \frac{h}{2}\tau_{yx,y}^{(n-1/2)}\right] - \delta_{nN}\left[\sigma_x^{(n+1/2)} + \frac{h}{2}\tau_{yx,y}^{(n+1/2)}\right] = 0, \tag{2a}$$

$$\tau_{xy}^{(n+1/2)} - \tau_{xy}^{(n-1/2)} + h\sigma_{y,y}^{(n)} + \delta_{n1}\tau_{xy}^{(n-1/2)} - \delta_{nN}\tau_{xy}^{(n+1/2)} = 0, \tag{2b}$$

for $n = 1, 2, \ldots, N$, where $\delta_{nm} \equiv$ Kronecker delta (i.e. $\delta_{nm} = 1$ if $n = m$, and $\delta_{nm} = 0$ otherwise), and the comma denotes partial differentiation.

By representing the x and y components of displacements as u and v, respectively, the constitutive equations for an orthotropic material can be written as

$$\sigma_x = C_{11}u_{,x} + C_{12}v_{,y}, \tag{3a}$$

$$\sigma_y = C_{12}u_{,x} + C_{22}v_{,y}, \tag{3b}$$

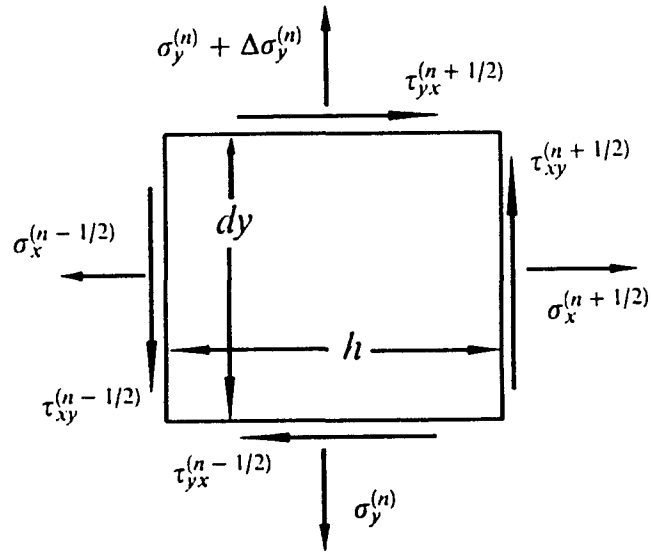

Fig. 3. Free-body diagram of a typical element used in COSL formulation.

$$\tau_{xy} = \tau_{yx} = C_{66}(u_{,y} + v_{,x}), \tag{3c}$$

where C_{ij} denotes the elastic constants.

The mid-node stresses can be approximated by averaging:

$$\sigma_x^{(n+1/2)} = \tfrac{1}{2}[\sigma_x^{(n+1/2)|^-} + \sigma_x^{(n+1/2)|^+}], \tag{4}$$

where the + and − denote stress values from the right and left, respectively. The aforementioned constitutive equations now become

$$\sigma_x^{(n+1/2)} = \tfrac{1}{2}\{[C_{11}^n u_{,x}^{(n+1/2)} + C_{12}^n v_{,y}^{(n+1/2)}]^- + [C_{11}^{n+1} u_{,x}^{(n+1/2)} + C_{12}^{n+1} v_{,y}^{(n+1/2)}]^+\}, \tag{5a}$$

$$\sigma_y^{(n)} = C_{12}^n u_{,x}^{(n)} + C_{22}^n v_{,y}^{(n)}, \tag{5b}$$

$$\tau_{xy}^{(n+1/2)} = \tfrac{1}{2}\{C_{66}^n [u_{,y}^{(n+1/2)} + v_{,x}^{(n+1/2)}]^- + C_{66}^{n+1}[u_{,y}^{(n+1/2)} + v_{,x}^{(n+1/2)}]^+\}. \tag{5c}$$

Define the displacement vectors to be

$$\mathbf{u} = \{u_1, u_2, \ldots, u_N\}^T, \tag{6a}$$

$$\mathbf{v} = \{v_1, v_2, \ldots, v_N\}^T. \tag{6b}$$

By using the above constitutive relation, eqn (5), in the equilibrium equation (2), and by converting to dimensionless form by letting $y = h\eta$, the following equations are obtained (Dharani and Tang, 1990):

$$\frac{d^2\mathbf{u}}{d\eta^2} - \mathbf{K}_u\mathbf{u} = \mathbf{C}_u \frac{d\mathbf{v}}{d\eta}, \tag{7a}$$

$$\frac{d^2\mathbf{v}}{d\eta^2} - \mathbf{K}_v\mathbf{v} = \mathbf{C}_v \frac{d\mathbf{u}}{d\eta}, \tag{7b}$$

where $\mathbf{K}_u$, $\mathbf{K}_v$, $\mathbf{C}_u$ and $\mathbf{C}_v$ are coefficient matrices given by Dharani and Tang (1990). These equations can be coupled into a single matrix equation by letting

$$\mathbf{w} = \{u_1, \ldots, u_N, v_1, \ldots, v_N, u_1', \ldots, u_N', v_1', \ldots, v_N'\}^T, \tag{8}$$

where the prime denotes differentiation with respect to η. The equation then becomes

$$\frac{d\mathbf{w}}{d\eta} = \mathbf{K}\mathbf{w}, \tag{9}$$

where

$$\mathbf{K} = \begin{bmatrix} \mathbf{O} & \mathbf{I} \\ \mathbf{K}_0 & \mathbf{C}_0 \end{bmatrix}, \quad \mathbf{I} = \text{identity matrix},$$

$$\mathbf{K}_0 = \begin{bmatrix} \mathbf{K}_u & \mathbf{O} \\ \mathbf{O} & \mathbf{K}_v \end{bmatrix} \quad \text{and} \quad \mathbf{C}_0 = \begin{bmatrix} \mathbf{O} & \mathbf{C}_u \\ \mathbf{C}_v & \mathbf{O} \end{bmatrix}.$$

The general solution of this set of equations can be found in terms of the eigenvalues and eigenvectors of $\mathbf{K}$, as in Dharani and Tang (1990). The derivation given up to this point was for all elements of equal width, h. By a slight modification, the equations can be given for non-uniform elements.

2.2. *Elastic mismatch*

For the bimaterial problem elastic mismatch can be quantified using Dundurs' (1969) parameters, α and β, which have been rewritten by He and Hutchinson (1989a) as

$$\alpha = \frac{\mu_2(1-\nu_1)-\mu_1(1-\nu_2)}{\mu_2(1-\nu_1)+\mu_1(1-\nu_2)} = \frac{\bar{E}_2-\bar{E}_1}{\bar{E}_2+\bar{E}_1}, \tag{10}$$

$$\beta = \frac{\mu_2(1-2\nu_1)-\mu_1(1-2\nu_2)}{\mu_2(1-\nu_1)+\mu_1(1-\nu_2)}, \tag{11}$$

where

$$\bar{E}_i = \frac{E_i}{1-\nu_i^2}.$$

μ_i denotes shear modulus, and ν_i denotes Poisson's ratio. It is important to note that the indices are the reverse of those used by He and Hutchinson (1989a). That is, $i = 1$ refers to the material containing the initial crack, and $i = 2$ refers to the material ahead of the crack.

2.3. *Energy release rates*

The stresses and displacements are computed from the formulation given above. To apply the crack penetration/deflection criterion given by eqn (1), the energy release rates for a penetrating crack (G_p) and a deflected crack (G_d) must be determined. For the penetrating crack, a potential energy approach is used [p. 159 of Kanninen and Popelar (1985)]. To employ this method, the potential energy, W, for a given crack configuration is defined as

$$W = \frac{1}{2}\sum_{i=1}^{N}(\sigma_y^{(i)}v_i h_i + \tau_{xy}^{(i)}u_i h_i). \tag{12}$$

The energy release rate is defined as

$$G_p = \frac{1}{2}\frac{\partial W}{\partial a}. \tag{13}$$

This expression is similar to eqn (3.3-3) of Kanninen and Popelar (1985), except that a factor of "2" is included to account for both crack tips. Using the finite-difference method, G_p can be approximated as

$$G_p = \frac{1}{2}\frac{\Delta W}{\Delta a} = \frac{W_2 - W_1}{2\Delta a}, \tag{14}$$

where a denotes crack length, W_1 denotes potential energy for a crack length a, and W_2 denotes potential energy for a crack of length $a+\Delta a$.

For the deflected crack, the energy release rate, G_d, is found by evaluating the crack closure integral of Irwin (1957), which has been recast as

$$G_d = \lim_{\delta\to 0}\left\{\frac{1}{2\delta}\left[\int_0^{\delta}\sigma_y(a,y)\bar{u}(a,y-\delta)\,dy + \int_0^{\delta}\tau_{xy}(a,y)\bar{v}(a,y-\delta)\,dy\right]\right\}, \tag{15}$$

where $\bar{u}$ and $\bar{v}$ denote relative displacements. In eqn (15), the first integral is for the contribution to G_d from Mode I, and the second integral is for the contribution to G_d from Mode II. It should be noted that G_d could have been found theoretically from the potential energy method used to find G_p. However, in computing values of G_d using both methods, the crack closure integral method produced more consistent results. This is due to the fact

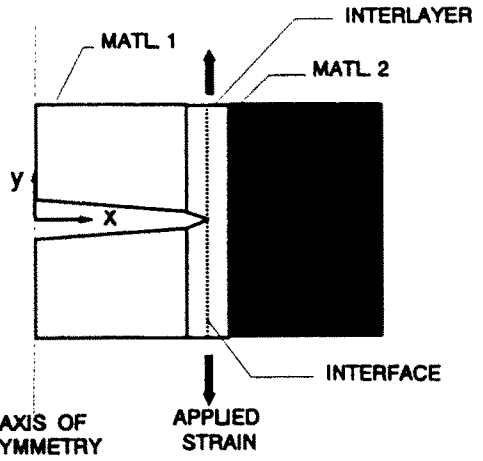

Fig. 4. Schematic of the interlayer at the bimaterial interface.

that the increment in split length was much smaller than the initial crack length, a. Since the potential energy method requires the two potential energies, W_1 and W_2, to be computed over the entire crack length, any difference due to the relatively small split length increment would be negligible. On the other hand, the crack closure integral method involves only the incremental split itself, without the initial crack. Therefore, the crack closure integral method is much more sensitive to changes in split length, and produces more consistent results.

2.4. *Interlayer model*

For the case of a crack occurring along a bimaterial interface, Sun and Manoharan (1989) and Yang (1991) observed that the crack-tip stress field exhibits a highly oscillatory behavior. This creates problems in defining the energy release rates for Mode I and Mode II. To alleviate this problem, it has been suggested by Raju *et al.* (1987) that an interlayer may be used at the interface itself. In a similar fashion, Yang (1991) uses such an interlayer to give a more gradual transition between the two regions of the bimaterial system.

In the present work, it has been observed that very high stress and displacement gradients occur near the interface. Although the geometry is quite different from the system studied by Yang (1991), it seems reasonable to use a similar interlayer to solve this problem. To implement the interlayer approach, the problem was modeled as shown in Fig. 4. As shown here, crack deflection is assumed to occur within the interlayer itself. Physically, this is analogous to a composite comprised of coated fibers in which fiber–matrix debonding occurs within the coating. To obtain material properties for the interlayer, the elastic constants C_{ij} for nodes adjacent to the interface were averaged, and these values were then substituted into the nodes comprising the interlayer. This allowed the interlayer to act as a buffer between the materials on either side of the interface. It is important to note that this approach gives reasonably good results as long as the interlayer is thin relative to the other regions. For the computations performed here, the interlayer had a thickness approximately 0.02 times the overall crack length.

3. RESULTS AND DISCUSSION

Since the computed values of G_d/G_p are found using a finite-difference formulation, the results may be dependent upon the number of nodes used. To determine what dependence, if any, exists, it is necessary to check the convergence of the results. Using properties for aluminum ($E = 69$ GPa and $\nu = 0.3$), the convergence was found by computing values of G_d/G_p for an increasing number of nodes. These results are given in Fig. 5. A uniform mesh (i.e. all elements of equal width) was used. To maintain a constant crack length, the nodal mesh size, h, was set equal to $1/N$, where N = the number of nodes. It was found that by letting the split (debond) length equal the mesh size, the convergence was quite acceptable.

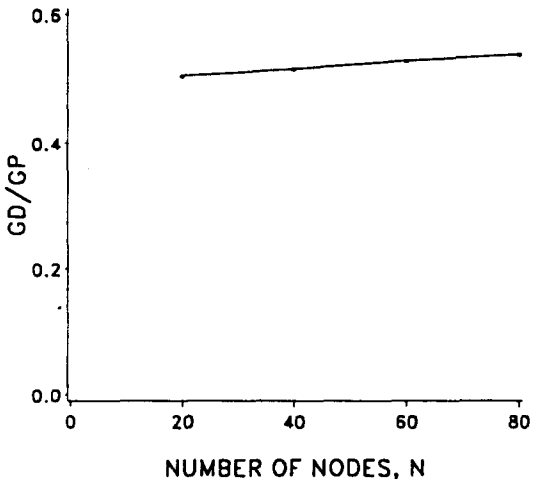

Fig. 5. Test of convergence of results for G_d/G_p.

Some results for the bimaterial arrangement shown in Fig. 1 are presented now. In such a bimaterial system, the two dissimilar elastic materials could be treated as homogeneous isotropic, homogeneous orthotropic, or heterogeneous, with a crack impinging perpendicularly upon the interface. The first case to be considered is that in which the two materials are homogeneous and isotropic. To fully investigate the effect of elastic mismatch upon G_d/G_p, it would be of interest to compute the ratio of energy release rates for various combinations of α and β. However, owing to the large amount of CPU time which would be required, the method here will be to calculate G_d/G_p versus α (holding β = constant), and similarly to calculate G_d/G_p versus β (holding α = constant). For the former (G_d/G_p vs α), the results are found for $\beta = 0$ and presented in Fig. 6. One curve is shown for the symmetric geometry described earlier, and corresponds to a matrix-crack lying between adjacent fibers in a fiber-reinforced composite. To give some sense of how these results compare with analytical results, the work of He and Hutchinson (1989a) is also shown. Since their results are valid for a system with only one interface, the previous COSL formulation was modified to allow for a free-edge along the y-axis (instead of a symmetric geometry), and these results are included for comparison. Of the two geometries studied here, the free-edge results show better agreement with the analytical results, especially for $\alpha > 0$. It should be noted that the bimaterial system studied by He and Hutchinson (1989a) consisted of semi-infinite elastic half-planes, whereas this research deals with a system of finite domains. Physically, an increase in α means that the material ahead of the crack tip becomes stiffer with respect to the material containing the crack. Consequently, as that

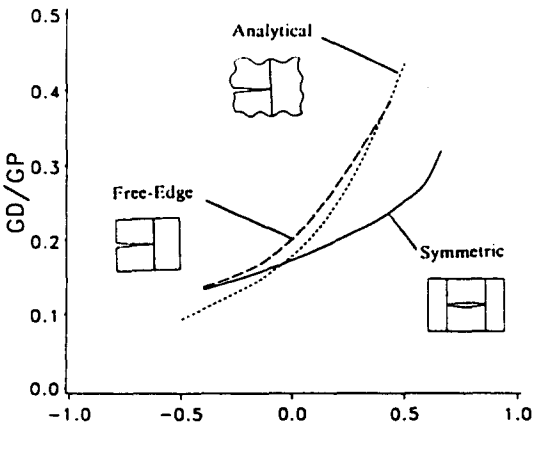

material becomes stiffer, the advancing crack has more tendency to deflect into the interface rather than penetrate the stiffer material. Thus, the trend shown in Fig. 6 makes physical sense. It is also worth noting that for $\alpha > 0$, the symmetric geometry predicts lower values for G_d/G_p than does the analytical model. One way of viewing these results is to apply them to fiber-reinforced composites. First assume that material 1 is the matrix, and let material 2 be the fiber. Since the analytical model is valid for semi-infinite regions, it can be viewed as a limiting case in which the fiber spacing is very high, and, therefore, the fiber volume fraction is very low. The COSL model, on the other hand, represents a more realistic composite with lower fiber spacing, and higher fiber volume fraction. In this manner, it can be argued that G_d/G_p decreases as fiber volume fraction increases (fiber spacing decreases), and this will indeed by shown in a later section.

One significant advantage of the present formulation is the relative ease with which Dundurs' second parameter, β, can be varied. In their work, He and Hutchinson (1989a, b) showed that for $\beta \neq 0$ the analytical formulation becomes much more complicated due to an oscillatory singularity. Fortunately, the COSL model does not have any such limitation. The results for G_d/G_p vs β ($\alpha = 0$) are shown in Fig. 7. It appears that the monotone decreasing trend shown is relatively slight compared to the effect of α on G_d/G_p. This result agrees with the argument of He and Hutchinson (1989b) that β is much less significant than α when these parameters are used to investigate crack-tip behavior in bimaterial systems.

One of the limitations of the present model is the manner in which the energy release rate for deflection, G_d, is found. That is, in order to compute this value, it is necessary to begin with a small initial split, or debond, length (theoretically, one should begin with an infinitesimal split length). As a result, the computed value of G_d depends on the split length chosen. To demonstrate this dependence, G_d/G_p was found for various values of split length using a uniform nodal mesh containing 80 nodes (40 nodes along the crack). The resultant graph of G_d/G_p vs debond length normalized with respect to crack length (l_d/a) is shown in Fig. 8. It is interesting to note that the ratio reaches a peak at a small value of normalized split length, $l_d/a \approx 0.01$, then gradually tapers off for larger values. For this reason, the results involving elastic mismatch, Figs 6 and 7, were computed using a normalized split length of 0.01. As it turns out, these results agree quite favorably with those of Budiansky *et al.* (1986). In particular, their results for debond length vs debond toughness demonstrate almost precisely the same behavior as that presented here. This is perhaps most surprising considering that the BHE model correctly accounts for the cylindrical geometry of the fiber, whereas the COSL model used here approximates each region, fiber or matrix, as a layer of uniform width. In their paper, Budiansky *et al.* (1986) also discuss the significance of G_d/G_p for values of l_d/a which occur between 0 and the peak value of G_d/G_p. They conclude that flaws and imperfections present within the matrix are likely to be large enough to preclude the existence of such small debonded lengths, which would imply that when

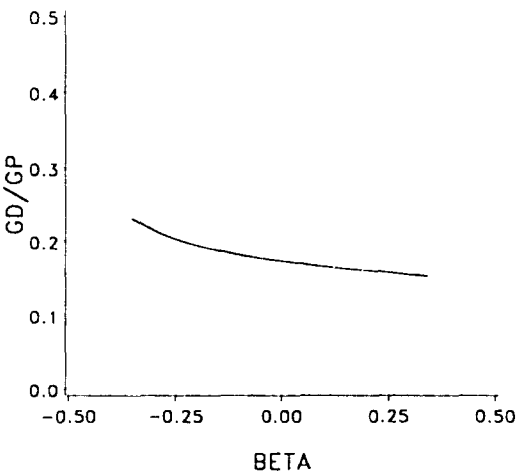

Fig. 7. Effect of Dundurs' parameter β on G_d/G_p, holding $\alpha = 0$.

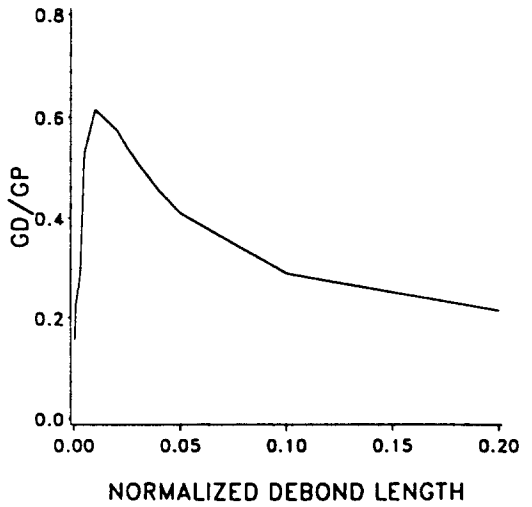

Fig. 8. Effect of normalized debond length (l_d/a) on G_d/G_p.

debonding occurs, the debonded length would immediately shift to a value to the right of the peak value of G_d/G_p.

The next results presented are intended to show what happens to the ratio G_d/G_p as the crack initially approaches the bimaterial interface and eventually penetrates it. The material properties used are $E_1 = 69$ GPa, $E_2 = 2E_1$, and $\nu_1 = \nu_2 = 0.3$. As it is used here, the normalized crack length, a/L, is defined so that $a/L = 1$ at the bimaterial interface. To obtain these results, debonding is assumed to occur at the crack tip, which is not always at the interface. It should be pointed out, however, that crack deflection (debonding) is unlikely until the crack tip reaches the interface. It is evident from Fig. 9 that the only significant effect on G_d/G_p is when the crack tip is very near the interface. This should probably come as no surprise since crack growth depends primarily upon the stress fields very near the crack tip itself, and therefore the interface appears to have little effect on cracks not directly impinging upon it.

In the analytical studies done on the bimaterial systems (He and Hutchinson, 1989a, b; Goree and Venezia, 1977a, b; Raju *et al.*, 1987; Rice, 1988; Sun and Manoharan, 1989; Yang, 1991), it was generally assumed that both materials were isotropic. Using the COSL approach, it is possible to generalize the bimaterial problem for those cases where one or both materials are anisotropic. As a means of demonstrating this, a system where the material behind the crack tip (material 1) is isotropic, and the material ahead of the crack tip (material 2) is anisotropic is considered. Material 1 was chosen to be aluminum, with

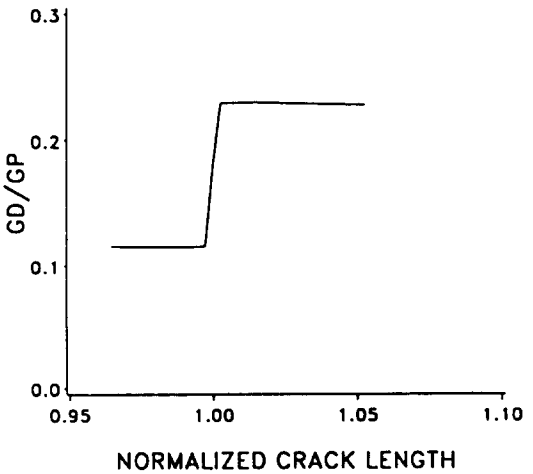

Fig. 9. Effect of normalized crack length (a/L) on G_d/G_p.

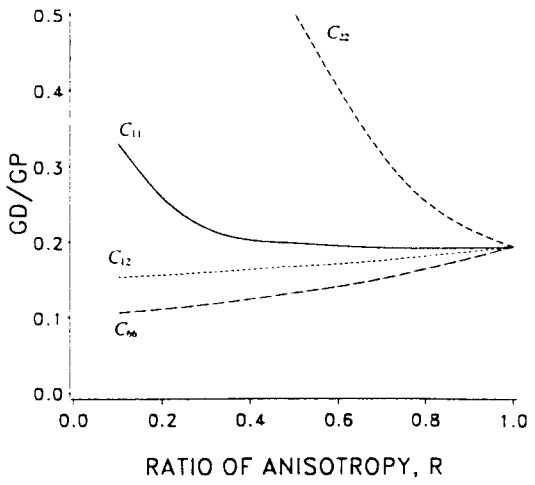

Fig. 10. Effect of anisotropy on G_d G_p.

$E_1 = 69$ GPa, and $\nu_1 = 0.35$, and material 2 was a hypothetical material with $E_2 = 20E_1$ and $\nu_2 = 0.30$. From these properties, the elastic constants, C_{ij}, were found. To create anisotropy in material 2, the original constants C_{ij} were modified so that one of them was varied while the others remained constant. To quantify this variation, the original C_{ij} value was multiplied by a "ratio of anisotropy", R. As an example, the curve for C_{11} was obtained by calculating G_d/G_p for RC_{11}, $0 < R \leqslant 1$, while C_{22}, C_{12} and C_{66} were kept unchanged. The results for various values of R are presented in Fig. 10. From these results, it is apparent that the energy release rate ratio is most greatly affected by C_{22}, and to a lesser extent by C_{11}. Conversely, the ratio is only slightly affected by C_{12} and C_{66}.

Since much interest in recent years has focussed on the use of CMCs, it is of some practical concern to investigate the behavior of crack growth in fiber–matrix composite systems. For these composites, the elastic moduli of the fiber and matrix phases are comparable, and the use of classical shear-lag models is unacceptable. In this paper, the COSL model is used to study the effect of fiber volume fraction on the ratio G_d/G_p. To accomplish this, the following typical properties that correspond to SiC/glass–ceramic composites are used: $E_m = 85$ GPa, $\nu_m = 0.25$, $E_f = 200$ GPa and $\nu_f = 0.25$. It should be pointed out that the model used here approximates each region, fiber and matrix, as a layer of uniform width, thus neglecting the cylindrical geometry of the fibers. Therefore, it is probably appropriate to consider the ratio of fiber width to fiber spacing to be an effective fiber volume fraction. By varying the number of nodes in each region, G_d/G_p is calculated for different volume fractions, and these values are given by Fig. 11. These results indicate

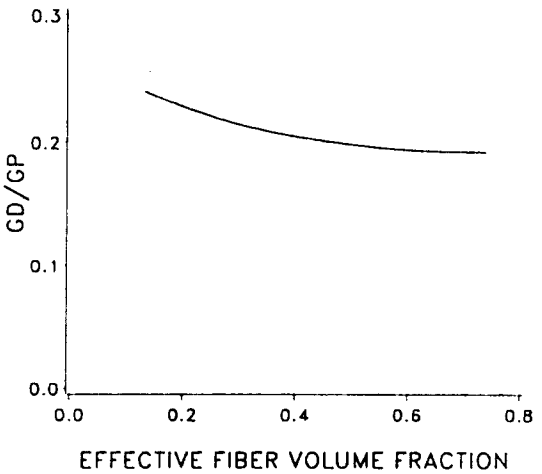

Fig. 11. Effect of fiber volume fraction, or fiber spacing, on G_d G_p.

that the energy release rate ratio shows a slight decrease for increasing V_f, although the effect is rather minimal. This could also be viewed as the variation of G_d/G_p as a function of fiber spacing for a given fiber size.

4. CONCLUSIONS

The results presented here demonstrate that the COSL model can be effectively used to predict the mode of extension, penetration or deflection, for cracks impinging upon a bimaterial interface. To facilitate the computations, an interlayer was included along the interface to act as a buffer between adjacent materials. By first using the COSL model to investigate the bimaterial problem, the subsequent results were shown to compare well with the existing analytical treatment of the same problem. In addition, the convergence was shown to be uniform and quite acceptable. Results are then presented for situations where the traditional analytical methods are not well suited, such as material anisotropy. It is shown that G_d/G_p is significantly affected by variations in C_{11} and C_{22}, whereas variations in C_{12} and C_{66} were of little consequence. For cracks at fiber–matrix interfaces in composite materials, the fiber volume fraction, or fiber spacing for a given fiber size, is shown to have relatively little effect on G_d/G_p.

Acknowledgement—The authors wish to acknowledge the Cornell National Supercomputing Facility (CNSF), whose resources were utilized extensively for the computational work involved in this research.

REFERENCES

Budiansky, B., Hutchinson, J. W. and Evans, A. G. (1986). Matrix fracture in fiber-reinforced ceramics. *J. Mech. Phys. Solids* **34**, 167–189.

Chai, L. and Dharani, L. R. (1991). Analysis of elastic crack bridging in ceramic matrix composites. *Theor. Appl. Fract. Mech.* **15**, 105–112.

Dharani, L. R., Jones, W. F. and Goree, J. G. (1983). Mathematical modeling of damage in unidirectional composites. *Engng Fract. Mech.* **17**, 555–573.

Dharani, L. R. and Recker, R. L. (1991). Growth of longitudinal damage in unidirectional composites. *Engng Fract. Mech.* **38**, 185–195.

Dharani, L. R. and Tang, H. (1990). Micromechanics characterization of sublaminate damage. *Int. J. Fract.* **46**, 123–140.

Dundurs, J. (1969). Edge-bonded dissimilar orthogonal elastic wedges under normal and shear loading. *J. Appl. Mech.* **36**, 650–652.

Goree, J. G. and Gross, R. S. (1979). Analysis of a unidirectional composite containing broken fibers and matrix damage. *Engng Fract. Mech.* **13**, 563–578.

Goree, J. G. and Venezia,W. A. (1977a). Bonded elastic half-planes with an interface crack and a perpendicular intersecting crack that extends into the adjacent material—I. *Int. J. Engng Sci.* **15**, 1–17.

Goree, J. G. and Venezia, W. A. (1977b). Bonded elastic half-planes with an interface crack and a perpendicular intersecting crack that extends into the adjacent material—II. *Int. J. Engng Sci.* **15**, 19–27.

He, M. Y. and Hutchinson, J. W. (1989a). Crack deflection at an interface between dissimilar elastic materials. *Int. J. Solids Structures* **25**(9), 1053–1067.

He, M. Y. and Hutchinson, J. W. (1989b). Kinking of a crack out of an interface. *J. Appl. Mech.* **56**, 270–278.

Hedgepeth, J. M. (1961). Stress concentrations in filamentary structures with broken fibers. NASA TN D-882.

Irwin, G. R. (1957). Analysis of stresses and strains near the end of a crack traversing a plate. *J. Appl. Mech.* **24**, 361–364.

Kanninen, M. F. and Popelar, C. H. (1985). *Advanced Fracture Mechanics*. Oxford University Press, New York.

Nairn, J. A. (1988). Fracture mechanics of unidirectional composites using the shear-lag model—I: theory. *J. Compos. Mater.* **22**, 561–588.

Nairn, J. A., Liu, S., Chen, H. and Wedgewood, A. R. (1991). Longitudinal splitting in epoxy and K-polymer composites: shear lag analysis including the effect of fiber bridging. *J. Compos. Mater.* **25**, 1086–1107.

Raju, I. S., Crews, J. H. and Aminpour, M. A. (1987). Convergence of strain energy release rate components for edge-delaminated composite laminates. NASA-TM 89135.

Rice, J. R. (1988). Elastic fracture mechanics concepts for interfacial cracks. *J. Appl. Mech.* **55**, 98–103.

Sun, C. T. and Manoharan, M. G. (1989). Interfacial crack between two orthotropic solids. *J. Compos. Mater.* **23**, 460–478.

Yang, W. (1991). New insights on interfacial fracture mechanics. *Proc. Joint FEFG/ICF International Conference on Fracture of Engineering Materials and Structures*, Singapore, 6–8 August 1991, pp. 51–56.